

Mohammad Arefi

# Analysis of wave in a functionally graded magneto-electro-elastic nano-rod using nonlocal elasticity model subjected to electric and magnetic potentials

Received: 29 November 2015 / Revised: 25 January 2016 / Published online: 10 May 2016  
© Springer-Verlag Wien 2016

**Abstract** The purpose of this research is to present the wave propagation analysis of a functionally graded nano-rod made of magneto-electro-elastic material subjected to an electric and magnetic potential. The unified nonlocal elasticity theory and Love's rod model are used in this study. All mechanical, electrical and magnetic properties are assumed to be variable along the thickness direction based on a power law distribution. Two-dimensional electric and magnetic potential distributions due to an applied potential and a magnet at the top of the rod are considered. The governing equations of motion are obtained using equilibrium and nonlocal theory of elasticity in conjunction with the Hamilton principle. The effect of important parameters of the functionally graded magneto-electro-elastic nano-rod such as nonlocal parameters, power index, wave number, applied magnetic and electric potentials on the wave propagation characteristics is studied.

## 1 Introduction

Local and nonlocal elasticity theories have been proposed for continuum media analysis in macro- and micro-nanoscales, respectively. The nonlocal theory states that the stress at a reference point depends not only on the strain at that point but also on the strains at all other points at the body. A nonlocal continuum mechanic model based on the Eringen's theory has been proposed for accounting the size dependency of very small structures [9]. In this paper, longitudinal wave propagation of a functionally graded piezomagnetic nano-rod subjected to two-dimensional electric and magnetic potentials has been carried out using a nonlocal model. The necessity of this study is clarified by performing a comprehensive literature review.

Ikeda [13] presented piezomagnetic analysis of magneto-elastic waves in a ferromagnetic thin film. The multi-field equations accounting for magneto-elastic behavior have been used for analysis of the wave propagation in the thin film. The obtained results have been confirmed with experiments. Kuo and Huang [15] presented a unified method based on the inclusion formulation for identification of the magnetic, electric, and elastic fields in a composite with piezoelectric and piezomagnetic phases. The effective magneto-electro-elastic constants such as elastic moduli, piezoelectric coefficients, dielectric constants, piezomagnetic coefficients, magnetoelectric, and magnetic permeability of the composites were expressed explicitly in terms of phase properties, volume fraction, and inhomogeneity shape. Ashida and Tauchert [5] presented wave propagation analysis of a circular piezoelectric plate subjected to one-dimensional heat conduction using the Laplace transform technique. The authors presented numerical results for two cases of piezoelectric and nonpiezoelectric materials. Hsu [12] studied electromechanical behavior of piezoelectric laminated composite beams using the differential quadrature method (DQM). The Chebyshev–Gauss–Lobatto sample point equation was used to select the sample points. The electromechanical responses of piezoelectric laminated composite beams with various boundary conditions were determined. He and Guan [11] studied the fundamental equations of the

M. Arefi (✉)

Department of Solid Mechanics, Faculty of Mechanical Engineering, University of Kashan, Kashan 87317-51167, Iran  
E-mail: arefi63@gmail.com; arefi@kashanu.ac.ir

space problem for transversely isotropy piezoelectric/piezomagnetic and elastic media. The multi-field equations were derived using the 3D elastic displacement, electric potential, and magnetic potential functions. Lu et al. [20] used the nonlocal plate model for the Kirchhoff and the Mindlin plate theories. The assumed theory was based on Eringen's theory of nonlocal continuum. Wang et al. [28] employed a nonlocal elasticity solution for evaluation of the length-dependent in-plane stiffness of achiral and chiral single-walled carbon nanotubes.

The wave propagating in 1D nanostructures with initial axial stress was investigated by Song et al. [26, 27]. They used a nonlocal elastic model incorporating with strain gradient theory. The governing equations for longitudinal and transverse waves in bars and beams have been derived using two scale parameters for introducing the size effect. The phase and group velocities of wave propagation were obtained analytically. Yan and Jiang [30] studied the surface effects on the vibration and buckling behavior of a simply supported piezoelectric nano-plate (PNP) by using a modified Kirchhoff plate model. Two kinds of in-plane constraints were defined for the PNP, and the surface effects were accounted for in the modified plate theory through the surface piezoelectricity model and the generalized Young–Laplace equations.

Wu and Hui [29] studied analytical and numerical solution of a nonlocal elastic bar in tension. Assadi and Farshi [6] studied the size-dependent free vibration analysis of nanotubes with surface effects. The Love's model of rods for study of longitudinal waves was employed. In order to simulate shear deformation, the Timoshenko beam model was used as supplementary analysis. Güven [19] considered the effect of initial stress on the wave propagation analysis of a nano-rod using a unified nonlocal model with two length scale parameters. The phase velocity of the nano-rod was derived explicitly in terms of nanoscale parameters, material properties and initial stress using Hamilton principle. Song et al. (2012) used a high-order continuum model and surface elasticity to study wave propagation in nano-wires. The results including phase velocity were evaluated in terms of different mechanical and nanoscale parameters. Ghorbanpour et al. [16] studied vibration analysis of the coupled system of double-layered graphene sheets (CS-DLGSs) embedded in a Visco-Pasternak foundation. The equation of motion was derived using the nonlocal elasticity theory of an orthotropic plate. Electro-thermal transverse vibration of fluid-conveying double-walled boron nitride nanotubes (DWBNTs) was studied by Ghorbanpour et al. [17]. The elastic medium was described by spring and van der Waals (vdW) forces between inner and outer nanotubes. Yan and Jiang [30] studied the surface effects on the vibration and buckling behavior of a simply supported piezoelectric nano-plate by using a modified Kirchhoff plate model. The stresses and strains of a functionally graded Timoshenko beam subjected to an arbitrary transverse loading were studied using the energy method by Hadi et al. [10].

A new higher-order shear deformation theory based on trigonometric shear deformation theory was developed for considering the size effects using the nonlocal elasticity theory by Nami and Janghorban [21]. Chen et al. [8] studied wave propagation analysis of a nano-sized, transversely isotropic cylinder. They used thin layer model to consider surface elasticity. They indicated that the surface effect has an important influence on the wave propagation of the nano-cylinder. Mohammadimehr and Rahmati [22] studied the electro-thermo-mechanical vibration analysis of nano-rod subjected to electric potential. They employed nonlocal elasticity theory for analysis. Güven [18] derived the equations of motion for one-dimensional wave propagation in a nano-bar. The phase velocities using the local and nonlocal solutions were calculated and compared in order to study the effect of the nonlocal parameter. Some electromechanical analyses of functionally graded piezoelectric materials have been performed by the author [1–4, 24].

The purpose of this study is to derive fundamental governing differential equations of wave propagation in a functionally graded magneto-electro-elastic nano-rod subjected to two-dimensional electric and magnetic potentials. For constituting the governing differential equations of the motion, a unified nonlocal elasticity model is used. Magneto-electro-elastic relations are used to account for the effect of multi-fields and nanoscale parameters on the nonlocal solutions of the nano-bar.

## 2 Formulation

### 2.1 Magnetoelectric fields

In this section, the basic relations of magneto-electro-elastic analysis are implemented. It is assumed that the nano-rod is made of magneto-electro-elastic materials. Three constitutive equations for identification of the structural behavior made of this material are expressed in vector form [7, 14, 25]:

$$\begin{aligned}
 T &= C\varepsilon - eE - dH, \\
 D &= e\varepsilon + \eta E + gH, \\
 B &= d\varepsilon + gE + \mu H,
 \end{aligned}
 \tag{1}$$

where  $T$  and  $\varepsilon$  are stress and strain tensors,  $E$  and  $D$  are electric field and electric displacement tensors,  $H$  and  $B$  are magnetic field and magnetic displacement components and  $C$ ,  $e$  and  $\eta$  are elastic stiffness, piezoelectric and dielectric tensors, respectively.  $d$ ,  $g$  and  $\mu$  are piezomagnetic, electromagnetic and magnetic coefficient tensors, respectively. The constitutive and piezoelectric relations are defined in terms of physical components as [25]:

$$\begin{aligned}
 T_{ij} &= C_{ijkl}\varepsilon_{kl} - e_{ijk}E_k - d_{ijk}H_k, \\
 D_i &= e_{ijk}\varepsilon_{jk} + \eta_{ik}E_k + g_{ik}H_k, \\
 B_i &= d_{ijk}\varepsilon_{jk} + g_{ik}E_k + \mu_{ik}H_k,
 \end{aligned}
 \tag{2}$$

where the components of the electric and magnetic fields  $E_k$ ,  $H_k$  are defined as:

$$\begin{aligned}
 E_k &= -\frac{\partial\phi}{\partial x_k}, \\
 H_k &= -\frac{\partial\Psi}{\partial x_k},
 \end{aligned}
 \tag{3}$$

where  $\phi$  and  $\Psi$  are the electric and magnetic potential. The magnetic and electric fields are introduced by considering the electric and magnetic potentials based on a two-dimensional electric potential as:

$$\begin{aligned}
 \Phi(x, z, t) &= \phi_1(x_3)\phi(x_1, t), \\
 \phi_1(x_3) &= \left(\frac{1}{2} + \frac{x_3}{h}\right)^e V_0, \quad e \geq 1,
 \end{aligned}
 \tag{4}$$

where  $V_0$  is an applied voltage at the top of the nano-rod and  $\left(\frac{1}{2} + \frac{z}{h}\right)^e$  is the assumed distribution for the electric potential along the transverse direction. For example,  $e=1$  is corresponding to a linear distribution and a greater value presents a higher-order distribution of the electric potential. Based on the assumed electric potential in Eq. (4), the electric field components are derived as [2,3]:

$$\begin{aligned}
 \Phi(x_1, x_3, t) &= \left(\frac{1}{2} + \frac{x_3}{h}\right)^e V_0\phi(x_1, t), \\
 E_1 &= -\frac{\partial\Phi}{\partial x_1} = -\left(\frac{1}{2} + \frac{x_3}{h}\right)^e V_0 \frac{\partial\phi(x_1, t)}{\partial x_1}, \\
 E_3 &= -\frac{\partial\Phi}{\partial x_3} = -\frac{e}{h} \left(\frac{1}{2} + \frac{x_3}{h}\right)^{e-1} V_0\phi(x_1, t).
 \end{aligned}
 \tag{5}$$

Similar to the electric potential, the magnetic potential of nano-rod is assumed as:

$$\begin{aligned}
 \Psi(x_1, x_3, t) &= \Psi_1(x_3)\Psi(x_1, t), \\
 \Psi_1(x_3) &= \left(\frac{1}{2} + \frac{x_3}{h}\right)^e H_0, \quad e \geq 1,
 \end{aligned}
 \tag{6}$$

where  $H_0$  is an applied magnetic field at the top of the plate and  $\left(\frac{1}{2} + \frac{x_3}{h}\right)^e$  is the assumed distribution for the magnetic potential along the transverse direction. The components of the magnetic field are derived using the gradient of Eq. (6) as follows:

$$\begin{aligned}
 \Psi(x_1, x_3, t) &= \left(\frac{1}{2} + \frac{x_3}{h}\right)^e V_0\Psi(x_1, t), \\
 E_1 &= -\frac{\partial\Psi}{\partial x_1} = -\left(\frac{1}{2} + \frac{x_3}{h}\right)^e H_0 \frac{\partial\Psi(x_1, t)}{\partial x_1}, \\
 E_3 &= -\frac{\partial\Psi}{\partial x_3} = -\frac{e}{h} \left(\frac{1}{2} + \frac{x_3}{h}\right)^{e-1} H_0\Psi(x_1, t).
 \end{aligned}
 \tag{7}$$

2.2 Displacement field and constitutive relations

Based on the Love’s rod model, we have the strain components as follows [18]:

$$\begin{cases} \varepsilon_{11} = \frac{\partial u(x_1,t)}{\partial x} \\ \varepsilon_{22} = \varepsilon_{33} = -\nu\varepsilon_{11} \end{cases} \tag{8}$$

where  $\varepsilon_{ij}$  are strain components,  $u(x_1, t)$  is the axial displacement and  $\nu$  is the Poisson ratio. Using the strain components defined in Eq. (8), the three displacement components are defined as:

$$\begin{cases} u(x_1, t) = u(x_1, t) \\ v(x_1, x_2, t) = -\nu x_2 \frac{\partial u(x_1,t)}{\partial x_1} \\ w(x_1, x_3, t) = -\nu x_3 \frac{\partial u(x_1,t)}{\partial x_1} \end{cases} \tag{9}$$

where  $u, v$  and  $w$  are the displacement components along the Cartesian coordinate axes  $x_1, x_2, x_3$ .

Linear strain–displacement relations in Cartesian coordinate system are defined as:

$$\begin{cases} \varepsilon_{xx} = \frac{\partial u}{\partial x_1} \\ \varepsilon_{yy} = \frac{\partial v}{\partial x_2} \\ \varepsilon_{zz} = \frac{\partial w}{\partial x_3} \end{cases}, \begin{cases} \varepsilon_{xy} = 1/2 \left( \frac{\partial u}{\partial x_2} + \frac{\partial v}{\partial x_1} \right) \\ \varepsilon_{xz} = 1/2 \left( \frac{\partial u}{\partial x_3} + \frac{\partial w}{\partial x_1} \right) \\ \varepsilon_{yz} = 1/2 \left( \frac{\partial v}{\partial x_3} + \frac{\partial w}{\partial x_2} \right) \end{cases} \tag{10}$$

Substitution of the displacement components from Eq. (9) into the strain displacement relations (10) yields the strain components in terms of the axial displacement  $u(x_1, t)$  as follows:

$$\begin{cases} \varepsilon_{xx} = \frac{\partial u(x_1,t)}{\partial x} \\ \varepsilon_{yy} = \frac{\partial v(x_1,x_2,t)}{\partial x_2} = -\nu \frac{\partial u(x_1,t)}{\partial x_1} \\ \varepsilon_{zz} = \frac{\partial w(x_1,x_3,t)}{\partial x_3} = -\nu \frac{\partial u(x_1,t)}{\partial x_1} \end{cases}, \begin{cases} \varepsilon_{xy} = 1/2 \left( \frac{\partial u}{\partial x_2} + \frac{\partial v}{\partial x_1} \right) = -1/2\nu x_2 \frac{\partial^2 u(x_1,t)}{\partial x_1^2} \\ \varepsilon_{xz} = 1/2 \left( \frac{\partial u}{\partial x_3} + \frac{\partial w}{\partial x_1} \right) = -1/2\nu x_3 \frac{\partial^2 u(x_1,t)}{\partial x_1^2} \\ \varepsilon_{yz} = 1/2 \left( \frac{\partial v}{\partial x_3} + \frac{\partial w}{\partial x_2} \right) = 0 \end{cases} \tag{11}$$

The stress components must be in dynamic equilibrium with the body and inertia forces:

$$\frac{\partial T_{ij}}{\partial x_j} + \rho B_i = \rho a_i \quad i = 1, 2, 3, \tag{12}$$

where  $T_{ij}$  and  $B_i$  are the components of the stress tensor and the body force,  $a_i$  are acceleration components and  $\rho$  is the density of the material. Extension of Eq. (12) in a three dimensional coordinate system with no body force effect gives:

$$\begin{cases} \frac{\partial T_{11}}{\partial x_1} + \frac{\partial T_{12}}{\partial x_2} + \frac{\partial T_{13}}{\partial x_3} = \rho \frac{\partial^2 u}{\partial t^2} \\ \frac{\partial T_{21}}{\partial x_1} + \frac{\partial T_{22}}{\partial x_2} + \frac{\partial T_{23}}{\partial x_3} = \rho \frac{\partial^2 v}{\partial t^2} \\ \frac{\partial T_{31}}{\partial x_1} + \frac{\partial T_{32}}{\partial x_2} + \frac{\partial T_{33}}{\partial x_3} = \rho \frac{\partial^2 w}{\partial t^2} \end{cases} \tag{13}$$

The generalized Hooke’s law using Lamé’s constants and considering electro-magneto effects yields the stress–strain relation as follows [1,4]:

$$T_{ij} = 2\mu\varepsilon_{ij} + \lambda\varepsilon_{kk}\delta_{ij} - e_{ijk}E_k - q_{ijk}H_k \rightarrow \begin{cases} T_{11} = E\varepsilon_{11} - e_{111}E_1 - e_{113}E_3 - q_{111}H_1 - q_{113}H_3 \\ T_{12} = -\mu\nu x_2 \frac{\partial^2 u}{\partial x_1^2} \\ T_{13} = -\mu\nu x_3 \frac{\partial^2 u}{\partial x_1^2} \end{cases} \tag{14}$$

where  $\mu$  and  $\lambda$  are Lamé constants,  $e_{ijk}$  are the piezoelectric constants,  $q_{ijk}$  the piezomagnetic coefficients,  $E_k$  is the electric field and  $H_k$  is the magnetic field. Substitution of the nonzero components of stress into the equations of motion (13) yields:

$$\begin{cases} \frac{\partial T_{11}}{\partial x_1} + \frac{\partial T_{12}}{\partial x_2} + \frac{\partial T_{13}}{\partial x_3} = \rho \frac{\partial^2 u}{\partial t^2} \\ \frac{\partial T_{21}}{\partial x_1} = \rho \frac{\partial^2 v}{\partial t^2} \\ \frac{\partial T_{31}}{\partial x_1} = \rho \frac{\partial^2 w}{\partial t^2} \end{cases} \tag{15}$$

The unified nonlocal elasticity model by considering the electric and magnetic effects is used as [18,21,23]

$$(1 - l_m^2 \nabla^2) T_{ij} = (1 - l_s^2 \nabla^2) (2\mu \varepsilon_{ij} + \lambda \varepsilon_{kk} \delta_{ij}) - e_{ijk} E_k - q_{ijk} H_k, \tag{16}$$

where  $\nabla^2$  is the Laplacian operator. Substitution of the nonzero components of stress and strain from the corresponding equations gives:

$$\begin{aligned} T_{11} - l_m^2 \frac{\partial^2 T_{11}}{\partial x_1^2} &= E \left( \varepsilon_{11} - l_s^2 \frac{\partial^2 \varepsilon_{11}}{\partial x_1^2} \right) - e_{111} E_1 - e_{113} E_3 - q_{111} H_1 - q_{113} H_3, \\ T_{12} - l_m^2 \frac{\partial^2 T_{12}}{\partial x_1^2} &= 2G \left( \varepsilon_{12} - l_s^2 \frac{\partial^2 \varepsilon_{12}}{\partial x_1^2} \right), \\ T_{13} - l_m^2 \frac{\partial^2 T_{13}}{\partial x_1^2} &= 2G \left( \varepsilon_{13} - l_s^2 \frac{\partial^2 \varepsilon_{13}}{\partial x_1^2} \right). \end{aligned} \tag{17}$$

For the derivation of the stress components from Eq. (17), it is necessary to evaluate the second derivative of the stress components using the equations of motion. For this purpose, one-time differentiation of Eq. (15) with respect to  $x_1, x_2, x_3$  should be performed. After these operations, we will have:

$$\begin{cases} \frac{\partial^2 T_{11}}{\partial x_1^2} + \frac{\partial^2 T_{12}}{\partial x_2 \partial x_1} + \frac{\partial^2 T_{13}}{\partial x_3 \partial x_1} = \rho \frac{\partial^3 u}{\partial x_1 \partial t^2} \\ \frac{\partial^2 T_{21}}{\partial x_2 \partial x_1} = \rho \frac{\partial^3 v}{\partial x_2 \partial t^2} \\ \frac{\partial^2 T_{31}}{\partial x_3 \partial x_1} = \rho \frac{\partial^3 w}{\partial x_3 \partial t^2} \end{cases} \tag{18}$$

By substitution of shear stress from the nonlocal form of Hooke’s law (18), we have:

$$\begin{cases} \frac{\partial^2 T_{11}}{\partial x_1^2} = \rho \frac{\partial^3 u}{\partial x_1 \partial t^2} - \frac{\partial^2 T_{12}}{\partial x_2 \partial x_1} - \frac{\partial^2 T_{13}}{\partial x_3 \partial x_1} \rightarrow \frac{\partial^2 T_{11}}{\partial x_1^2} = \rho(1 + \nu) \frac{\partial^3 u(x_1, t)}{\partial x_1 \partial t^2} + \frac{\partial(\rho \nu x_3)}{\partial x_3} \frac{\partial^3 u(x_1, t)}{\partial x_1 \partial t^2} \\ \frac{\partial^2 T_{21}}{\partial x_2 \partial x_1} = \frac{\partial}{\partial x_2} \left\{ \rho \frac{\partial^2 v}{\partial t^2} \right\} = \frac{\partial}{\partial x_2} \left\{ \rho \frac{\partial^2 v}{\partial t^2} \right\} = -\rho \nu \frac{\partial^3 u(x_1, t)}{\partial x_1 \partial t^2} \\ \frac{\partial^2 T_{31}}{\partial x_3 \partial x_1} = \frac{\partial}{\partial x_3} \left\{ \rho \frac{\partial^2 w}{\partial t^2} \right\} = -\frac{\partial}{\partial x_3} \left\{ \rho \nu x_3 \frac{\partial^3 u(x_1, t)}{\partial x_1 \partial t^2} \right\} \end{cases} \tag{19}$$

After appropriate changes and some simplifications, we have:

$$\begin{cases} \frac{\partial^2 T_{11}}{\partial x_1^2} = \left\{ \rho(1 + 2\nu) + \nu x_3 \frac{\partial \rho}{\partial x_3} \right\} \frac{\partial^3 u(x_1, t)}{\partial x_1 \partial t^2} \\ \frac{\partial^2 T_{21}}{\partial x_2 \partial x_1} = -\rho \nu \frac{\partial^3 u(x_1, t)}{\partial x_1 \partial t^2} \\ \frac{\partial^2 T_{31}}{\partial x_3 \partial x_1} = -\frac{\partial}{\partial x_3} \left\{ \rho \nu x_3 \frac{\partial^3 u(x_1, t)}{\partial x_1 \partial t^2} \right\} \end{cases} \tag{20}$$

Finally, three components of stress in terms of displacement components and electric and magnetic functions are derived as:

$$\begin{cases} T_{11} = l_m^2 \left\{ \rho(1 + 2\nu) + \nu x_3 \frac{\partial \rho}{\partial x_3} \right\} \frac{\partial^3 u(x_1, t)}{\partial x_1 \partial t^2} + E \left( \frac{\partial u(x_1, t)}{\partial x_1} - l_s^2 \frac{\partial^3 u(x_1, t)}{\partial x_1^3} \right) + e_{111} \left( \frac{1}{2} + \frac{x_3}{h} \right)^e V_0 \frac{\partial \phi(x_1)}{\partial x_1} \\ \quad + e_{113} \frac{e}{h} \left( \frac{1}{2} + \frac{x_3}{h} \right)^{e-1} V_0 \phi(x_1) + q_{111} \left( \frac{1}{2} + \frac{x_3}{h} \right)^e H_0 \frac{\partial \Psi(x_1)}{\partial x_1} + q_{113} \frac{e}{h} \left( \frac{1}{2} + \frac{x_3}{h} \right)^{e-1} H_0 \Psi(x_1) \\ T_{21} = -l_m^2 \rho \nu x_2 \frac{\partial^4 u(x_1, t)}{\partial x_1^2 \partial t^2} + \frac{E}{2(1+\nu)} \nu x_2 \left\{ -\frac{\partial^2 u(x_1, t)}{\partial x_1^2} + l_s^2 \frac{\partial^4 u(x_1, t)}{\partial x_1^4} \right\} \\ T_{13} = -l_m^2 \rho \nu x_3 \frac{\partial^3 u(x_1, t)}{\partial x_1^2 \partial t^2} + \frac{E}{2(1+\nu)} \nu x_3 \left\{ -\frac{\partial^2 u(x_1, t)}{\partial x_1^2} + l_s^2 \frac{\partial^4 u(x_1, t)}{\partial x_1^4} \right\} \end{cases} \tag{21}$$

For an electromechanical system, electric displacement is defined as [2–4,24]:

$$\begin{aligned}
 D_i &= e_{ijk}\varepsilon_{jk} + \eta_{ik}E_k + g_{ik}H_k, \\
 D_1 &= e_{111}\varepsilon_{11} + \eta_{11}E_1 + \eta_{13}E_3 + g_{11}H_1 + g_{13}H_3 = e_{111}\frac{\partial u(x_1, t)}{\partial x_1} - \eta_{11}\left(\frac{1}{2} + \frac{x_3}{h}\right)^e V_0\frac{\partial\phi(x_1, t)}{\partial x_1} \\
 &\quad - \eta_{13}\frac{e}{h}\left(\frac{1}{2} + \frac{x_3}{h}\right)^{e-1} V_0\phi(x_1, t) - g_{11}\left(\frac{1}{2} + \frac{x_3}{h}\right)^e H_0\frac{\partial\Psi(x_1, t)}{\partial x_1} - g_{13}\frac{e}{h}\left(\frac{1}{2} + \frac{x_3}{h}\right)^{e-1} H_0\Psi(x_1, t), \\
 D_3 &= e_{311}\varepsilon_{11} + \eta_{31}E_1 + \eta_{33}E_3 + g_{31}H_1 + g_{33}H_3 = e_{311}\frac{\partial u(x_1, t)}{\partial x_1} - \eta_{31}\left(\frac{1}{2} + \frac{x_3}{h}\right)^e V_0\frac{\partial\phi(x_1, t)}{\partial x_1} \\
 &\quad - \eta_{33}\frac{e}{h}\left(\frac{1}{2} + \frac{x_3}{h}\right)^{e-1} V_0\phi(x_1, t) - g_{31}\left(\frac{1}{2} + \frac{x_3}{h}\right)^e H_0\frac{\partial\Psi(x_1, t)}{\partial x_1} - g_{33}\frac{e}{h}\left(\frac{1}{2} + \frac{x_3}{h}\right)^{e-1} H_0\Psi(x_1, t).
 \end{aligned} \tag{22}$$

Therefore, the magnetic induction components are derived as follows:

$$\begin{aligned}
 B_i &= q_{ijk}\varepsilon_{jk} + g_{ik}E_k + \mu_{ik}H_k, \\
 B_1 &= q_{111}\varepsilon_{11} + g_{11}E_1 + g_{13}E_3 + \mu_{11}H_1 + \mu_{13}H_3 = q_{111}\frac{\partial u(x_1, t)}{\partial x_1} - g_{11}\left(\frac{1}{2} + \frac{x_3}{h}\right)^e V_0\frac{\partial\phi(x_1, t)}{\partial x_1} \\
 &\quad - g_{13}\frac{e}{h}\left(\frac{1}{2} + \frac{x_3}{h}\right)^{e-1} V_0\phi(x_1, t) - \mu_{11}\left(\frac{1}{2} + \frac{x_3}{h}\right)^e H_0\frac{\partial\Psi(x_1, t)}{\partial x_1} - \mu_{13}\frac{e}{h}\left(\frac{1}{2} + \frac{x_3}{h}\right)^{e-1} H_0\Psi(x_1, t), \\
 B_3 &= q_{311}\varepsilon_{11} + g_{31}E_1 + g_{33}E_3 + \mu_{31}H_1 + \mu_{33}H_3 = q_{311}\frac{\partial u(x_1, t)}{\partial x_1} - g_{31}\left(\frac{1}{2} + \frac{x_3}{h}\right)^e V_0\frac{\partial\phi(x_1, t)}{\partial x_1} \\
 &\quad - g_{33}\frac{e}{h}\left(\frac{1}{2} + \frac{x_3}{h}\right)^{e-1} V_0\phi(x_1, t) - \mu_{31}\left(\frac{1}{2} + \frac{x_3}{h}\right)^e H_0\frac{\partial\Psi(x_1, t)}{\partial x_1} - \mu_{33}\frac{e}{h}\left(\frac{1}{2} + \frac{x_3}{h}\right)^{e-1} H_0\Psi(x_1, t).
 \end{aligned} \tag{23}$$

The required material properties defined in these relations are inhomogeneous along the thickness direction. Based on this assumption, for a symbolic material property  $\Upsilon(x_3)$ , we have following functionality:

$$\Upsilon(x_3) = (\Upsilon_t - \Upsilon_b)\left(\frac{1}{2} + \frac{x_3}{h}\right)^n + \Upsilon_b, \tag{24}$$

where  $\Upsilon_t$ ,  $\Upsilon_b$  are material properties at top and bottom, respectively,  $n$  is the power index, and  $2h$  is the thickness of the nano-rod. After derivation of mechanical and electrical components (stress, strain, electric and magnetic fields, electric and magnetic displacements), Hamilton's principle is used for derivation of the total energy of the nano-rod and consequently governs the differential equations of the system.

The kinetic energy of the nano-rod is obtained as follows:

$$\begin{aligned}
 KE &= \int \int \int \frac{1}{2}\rho \{\dot{u}^2 + \dot{v}^2 + \dot{w}^2\} dx_1 dx_2 dx_3 = \int \int \int \frac{1}{2}\rho \left\{ \left(\frac{\partial u(x_1, t)}{\partial t}\right)^2 + \left(\nu_{x_2}\frac{\partial^2 u(x_1, t)}{\partial t \partial x_1}\right)^2 \right. \\
 &\quad \left. + \left(\nu_{x_3}\frac{\partial^2 u(x_1, t)}{\partial t \partial x_1}\right)^2 \right\} dx_1 dx_2 dx_3.
 \end{aligned} \tag{25}$$

The strain energy of the system is

$$U = \int \int \int \frac{1}{2}\{T_{11}\varepsilon_{11} + 2T_{12}\varepsilon_{12} + 2T_{13}\varepsilon_{13} - D_1E_1 - D_3E_3 - B_1H_1 - B_3H_3\} dx_1 dx_2 dx_3. \tag{26}$$

Substitution of the required equations for stress, strain, electric displacement and electric field from Eqs. (11, 21, 22, 23) gives the strain energy as follows:

$$\begin{aligned}
 U = & \iiint \frac{1}{2} \left\{ \left[ l_m^2 \left\{ \rho(1 + 2\nu) + \nu x_3 \frac{\partial \rho}{\partial x_3} \right\} \frac{\partial^3 u(x_1, t)}{\partial x_1 \partial t^2} + E \left( \frac{\partial u(x_1, t)}{\partial x_1} - l_s^2 \frac{\partial^3 u(x_1, t)}{\partial x_1^3} \right) + e_{111} \left( \frac{1}{2} + \frac{z}{h} \right)^e V_0 \frac{\partial \phi(x_1, t)}{\partial x_1} \right. \right. \\
 & \left. \left. + e_{113} \frac{e}{h} \left( \frac{1}{2} + \frac{z}{h} \right)^{e-1} V_0 \phi(x_1, t) + q_{111} \left( \frac{1}{2} + \frac{z}{h} \right)^e H_0 \frac{\partial \psi_2(x_1, t)}{\partial x_1} + q_{113} \frac{e}{h} \left( \frac{1}{2} + \frac{z}{h} \right)^{e-1} H_0 \psi_2(x_1, t) \right] \frac{\partial u(x_1, t)}{\partial x_1} \right. \\
 & + \left[ -l_m^2 \rho \nu x_2 \frac{\partial^4 u(x_1, t)}{\partial x_1^2 \partial t^2} + \frac{E}{2(1 + \nu)} \left\{ -\nu x_2 \frac{\partial^2 u(x_1, t)}{\partial x_1^2} + l_s^2 \nu x_2 \frac{\partial^4 u(x_1, t)}{\partial x_1^4} \right\} \right] \left[ -\nu x_2 \frac{\partial^2 u(x_1, t)}{\partial x^2} \right] \\
 & + \left[ -l_m^2 \rho \nu x_3 \frac{\partial^4 u(x_1, t)}{\partial x_1^2 \partial t^2} + \frac{E}{2(1 + \nu)} \left\{ -\nu x_3 \frac{\partial^2 u(x_1, t)}{\partial x_1^2} + l_s^2 \nu x_3 \frac{\partial^4 u(x_1, t)}{\partial x_1^4} \right\} \right] \left[ -\nu x_3 \frac{\partial^2 u(x_1, t)}{\partial x^2} \right] \\
 & + \left[ e_{111} \frac{\partial u(x_1, t)}{\partial x_1} - \eta_{11} \left( \frac{1}{2} + \frac{z}{h} \right)^e V_0 \frac{\partial \phi(x_1, t)}{\partial x_1} - \eta_{13} \frac{e}{h} \left( \frac{1}{2} + \frac{z}{h} \right)^{e-1} V_0 \phi(x_1, t) - g_{11} \left( \frac{1}{2} + \frac{z}{h} \right)^e H_0 \frac{\partial \psi_2(x_1, t)}{\partial x_1} \right. \\
 & \left. - g_{13} \frac{e}{h} \left( \frac{1}{2} + \frac{z}{h} \right)^{e-1} H_0 \psi_2(x_1, t) \right] \left( \frac{1}{2} + \frac{z}{h} \right)^e V_0 \frac{\partial \phi(x_1, t)}{\partial x_1} + \left[ e_{311} \frac{\partial u(x_1, t)}{\partial x_1} - \eta_{31} \left( \frac{1}{2} + \frac{z}{h} \right)^e V_0 \frac{\partial \phi(x_1, t)}{\partial x_1} \right. \\
 & \left. - \eta_{33} \frac{e}{h} \left( \frac{1}{2} + \frac{z}{h} \right)^{e-1} V_0 \phi(x_1, t) - g_{31} \left( \frac{1}{2} + \frac{z}{h} \right)^e H_0 \frac{\partial \psi_2(x_1, t)}{\partial x_1} - g_{33} \frac{e}{h} \left( \frac{1}{2} + \frac{z}{h} \right)^{e-1} H_0 \psi_2(x_1, t) \right] \\
 & \times \frac{e}{h} \left( \frac{1}{2} + \frac{z}{h} \right)^{e-1} V_0 \phi(x_1, t) + \left[ q_{111} \frac{\partial u(x_1, t)}{\partial x_1} - g_{11} \left( \frac{1}{2} + \frac{z}{h} \right)^e V_0 \frac{\partial \phi(x_1, t)}{\partial x_1} - g_{13} \frac{e}{h} \left( \frac{1}{2} + \frac{z}{h} \right)^{e-1} V_0 \phi(x_1, t) \right. \\
 & \left. - \mu_{11} \left( \frac{1}{2} + \frac{z}{h} \right)^e H_0 \frac{\partial \psi_2(x_1, t)}{\partial x_1} - \mu_{13} \frac{e}{h} \left( \frac{1}{2} + \frac{z}{h} \right)^{e-1} H_0 \psi_2(x_1, t) \right] \left( \frac{1}{2} + \frac{z}{h} \right)^e H_0 \frac{\partial \psi_2(x_1, t)}{\partial x_1} \\
 & + \left[ q_{311} \frac{\partial u(x_1, t)}{\partial x_1} - g_{31} \left( \frac{1}{2} + \frac{z}{h} \right)^e V_0 \frac{\partial \phi(x_1, t)}{\partial x_1} - g_{33} \frac{e}{h} \left( \frac{1}{2} + \frac{z}{h} \right)^{e-1} V_0 \phi(x_1, t) - \mu_{31} \left( \frac{1}{2} + \frac{z}{h} \right)^e H_0 \frac{\partial \psi_2(x_1, t)}{\partial x_1} \right. \\
 & \left. - \mu_{33} \frac{e}{h} \left( \frac{1}{2} + \frac{z}{h} \right)^{e-1} H_0 \psi_2(x_1, t) \right] \frac{e}{h} \left( \frac{1}{2} + \frac{z}{h} \right)^{e-1} H_0 \psi_2(x_1, t) \Big\} dx_1 dx_2 dx_3. \tag{27}
 \end{aligned}$$

In order to obtain final equations of motion, Hamilton’s principle is used as

$$\int_{t_1}^{t_2} (\delta KE - \delta U) dt = 0. \tag{28}$$

Considering the variation of the kinetic and the potential energy in Hamilton’s principle and performing integration by part yields three governing differential equations of motion in terms of the coefficients of  $\delta u, \delta \phi, \delta \Psi$  as follows:

$$\begin{aligned}
 \delta u: & -A \frac{\partial^2 u}{\partial t^2} + B \frac{\partial^4 u}{\partial t^2 \partial x_1^2} + C \frac{\partial^4 u}{\partial x_1^2 \partial t^2} + D \frac{\partial^2 u}{\partial x_1^2} + E \frac{\partial^4 u}{\partial x_1^4} + F \frac{\partial^2 \phi}{\partial x_1^2} + G \frac{\partial \phi}{\partial x_1} - H \frac{\partial^6 u}{\partial x_1^4 \partial t^2} \\
 & - I \frac{\partial^4 u}{\partial x_1^4} - J \frac{\partial^6 u}{\partial x_1^6} + P \frac{\partial^2 \Psi}{\partial x_1^2} + Q \frac{\partial \Psi}{\partial x_1} = 0, \\
 \delta \phi: & K \frac{\partial^2 u}{\partial x_1^2} - O \frac{\partial u}{\partial x_1} + L \frac{\partial^2 \phi}{\partial x_1^2} + N \frac{\partial \phi}{\partial x_1} - M \phi + S \frac{\partial \Psi}{\partial x_1} + U \Psi = 0, \\
 \delta \Psi: & W \frac{\partial^2 u}{\partial x_1^2} + X \frac{\partial^2 \phi}{\partial x_1^2} + Y \frac{\partial \phi}{\partial x_1} + Z \frac{\partial^2 \Psi}{\partial x_1^2} + A_1 \frac{\partial \Psi}{\partial x_1} + C_1 \frac{\partial u}{\partial x_1} + D_1 \frac{\partial \phi}{\partial x_1} + E_1 \phi + F_1 \frac{\partial \Psi}{\partial x_1} + G_1 \Psi = 0, \tag{29}
 \end{aligned}$$

where all integration constants  $A, B, \dots, Z$  and  $A_1 \dots G_1$  are expressed in the Appendix. Considering the harmonic longitudinal wave propagation equation and harmonic electric and magnetic potentials along the

longitudinal direction using  $u(x_1, t) = U e^{ik(x_1-ct)}$ ,  $\phi(x_1, t) = \Phi e^{ik(x_1-ct)}$ ,  $\Psi(x_1, t) = \Psi e^{ik(x_1-ct)}$  and substitution into the governing differential equation yields [26,27]

$$\begin{bmatrix} \chi_{11} & \chi_{12} & \chi_{13} \\ \chi_{21} & \chi_{22} & \chi_{23} \\ \chi_{31} & \chi_{32} & \chi_{32} \end{bmatrix} \begin{Bmatrix} U \\ \Phi \\ \Psi \end{Bmatrix} = \begin{Bmatrix} 0 \\ 0 \\ 0 \end{Bmatrix}, \tag{30}$$

where  $\chi_{ij}$  are functions of integration constants shown in the Appendix,  $k$  is the wave number, and  $c$  is the phase velocity. To obtain the velocity of wave propagation, the determinant of the matrix  $[\chi_{ij}]$  must be considered zero.

### 3 Numerical results and discussion

The numerical results of the problem are calculated using the determinant of the matrix  $[\chi_{ij}]$  derived in Eq. (30) in terms of different parameters of the electro-magneto-mechanical system. The obtained results

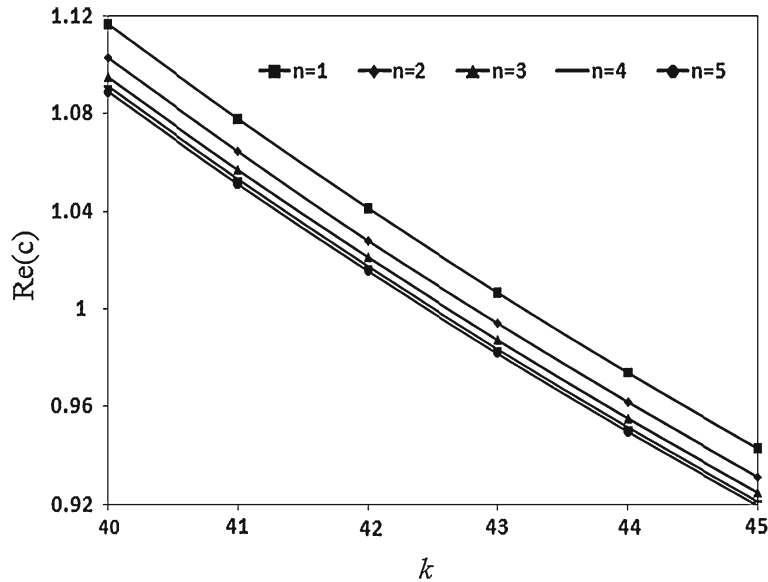


Fig. 1 Dimensionless real part of  $c$  in terms of wave number for different values of power index for  $V_0 = 5$  V and  $H_0 = 5$  A

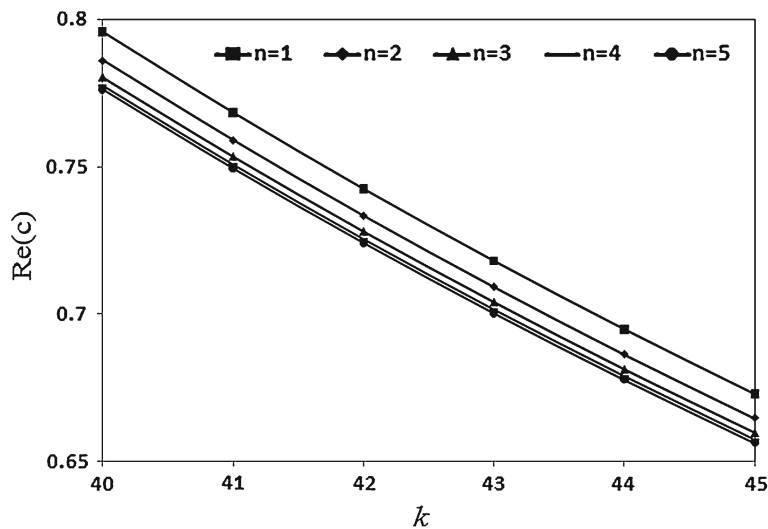


Fig. 2 Dimensionless real part of  $c$  in terms of wave number for different values of power index for  $V_0 = 10$  V and  $H_0 = 10$  A



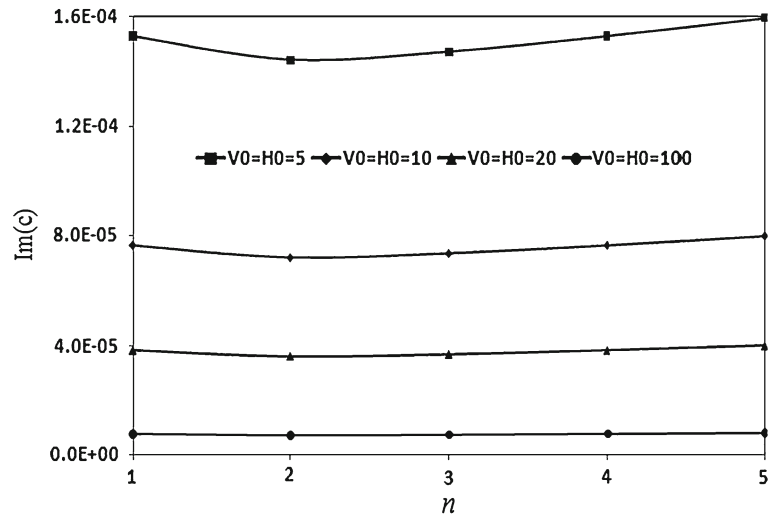


Fig. 3 Real part of  $c$  in terms of power index for different applied voltage and magnetic

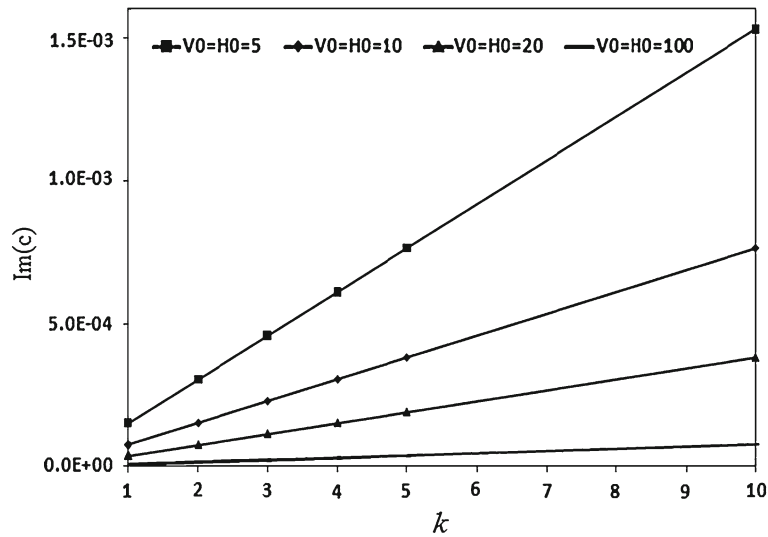


Fig. 4 Imaginary part of  $c$  in terms of power index for different applied voltage

contain real and imaginary parts of  $c$ . These results are presented in terms of power index  $n$ , wave number  $k$  and applied magnetic field and voltage  $H_0, V_0$ . The dimension of the cross section of the nano-rod is assumed as  $b = h = 1$  nm. The numerical values of the material constants are stated as:

$$\rho = 5500 \frac{\text{kg}}{\text{m}^3}, \nu = 0.3, E = 226 \text{ GPa}, e_{111} = 9.3 \frac{\text{C}}{\text{m}^2}, e_{113} = -2.2 \frac{\text{C}}{\text{m}^2},$$

$$q_{113} = 290, q_{333} = 350, \eta_{11} = 5.64 \times 10^{-9} \frac{\text{C}}{\text{mV}},$$

$$\eta_{33} = 6.35 \times 10^{-9} \frac{\text{C}}{\text{mV}}, g_{13} = 5.37 \times 10^{-12} \frac{\text{Ns}}{\text{CV}}, g_{33} = 2737 \times 10^{-12} \frac{\text{Ns}}{\text{CV}},$$

$$\mu_{11} = -297 \times 10^{-6} \frac{\text{Ns}^2}{\text{C}^2}, \mu_{13} = 83 \times 10^{-6} \frac{\text{Ns}^2}{\text{C}^2}.$$

Shown in Fig. 1 is the distribution of the dimensionless real part of the phase velocity  $c$  in terms of the wave number for different values of the power index for  $V_0 = 5$  V and  $H_0 = 5$  A. It is concluded that with increasing the wave number, the real part of  $c$  decreases considerably. Furthermore, investigation on the effect

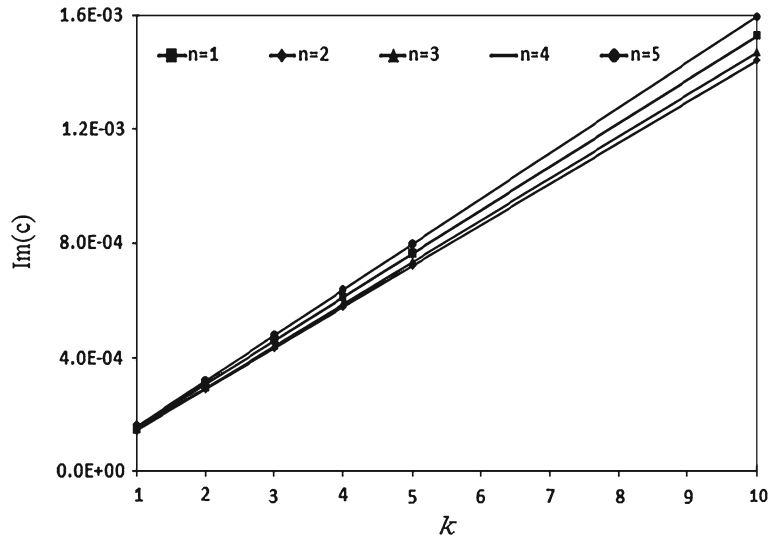


Fig. 5 Dimensionless imaginary part of  $c$  in terms of wave number for different power index for  $V_0 = 10$  V and  $H_0 = 10$  A

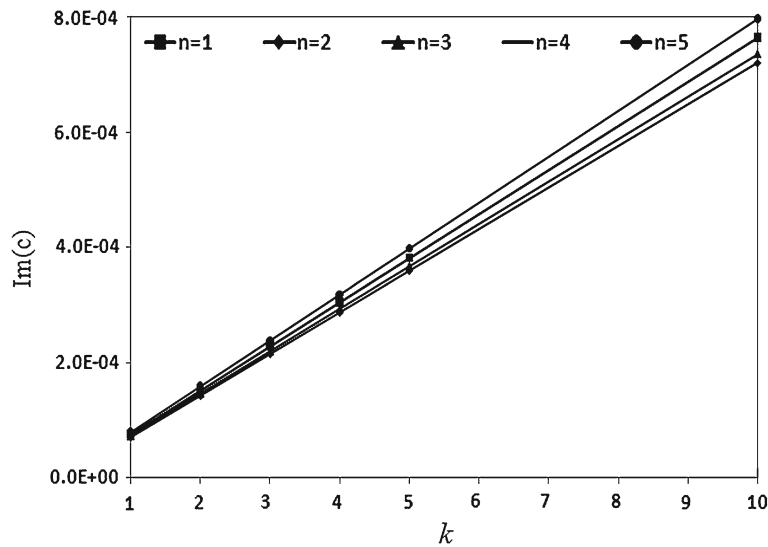


Fig. 6 Dimensionless imaginary part of  $c$  in terms of wave number for different power index for  $V_0 = 5$  V and  $H_0 = 5$  A

of power index  $n$  indicates that with increasing the power index, the phase velocity decreases. This decreasing is due to decreasing the stiffness of materials.

Shown in Fig. 2 is the distribution of the dimensionless real part of the phase velocity  $c$  in terms of the wave number for different values of the power index for  $V_0 = 10$  V and  $H_0 = 10$  A. Decreasing phase velocity  $c$ , with increasing power index  $n$  and wave number  $k$ , is concluded from Fig. 2.

Figure 3 shows the distribution of the dimensionless imaginary part of the phase velocity  $c$  in terms of the power index  $n$ , for different values of applied magnetic and voltage. It can be concluded that with increasing applied voltage and magnetic field, the imaginary part of the phase velocity decreases considerably.

The other important results of Fig. 3 are that the distribution of the imaginary part for different values of the power index has a minimum value for  $n = 2$ .

Figure 4 shows the distribution of the dimensionless imaginary part of the phase velocity  $c$  in terms of the wave number for different values of applied voltage and magnetic field. It can be concluded that with increasing applied voltage and magnetic field and wave number, the imaginary part decreases considerably.

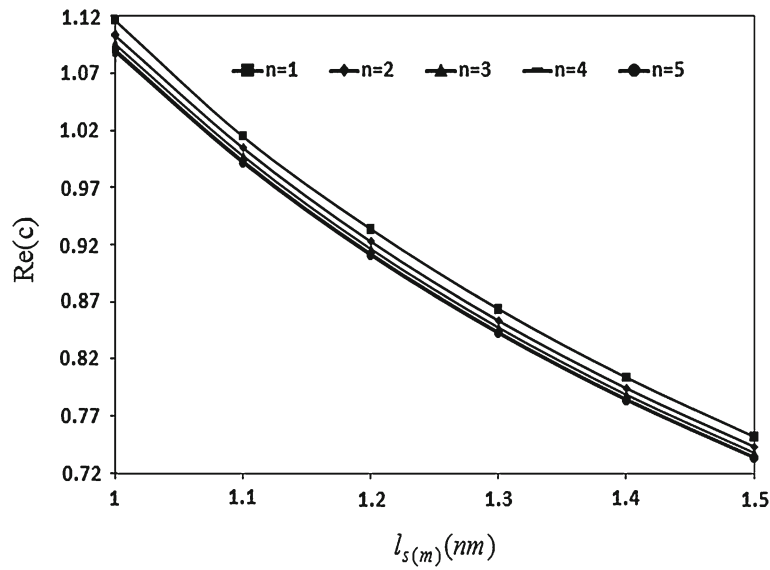


**Fig. 7** Dimensionless real part of  $c$  in terms of nonlocal parameter of nano-rod for different power index for  $V_0 = 5$  V and  $H_0 = 5$  A

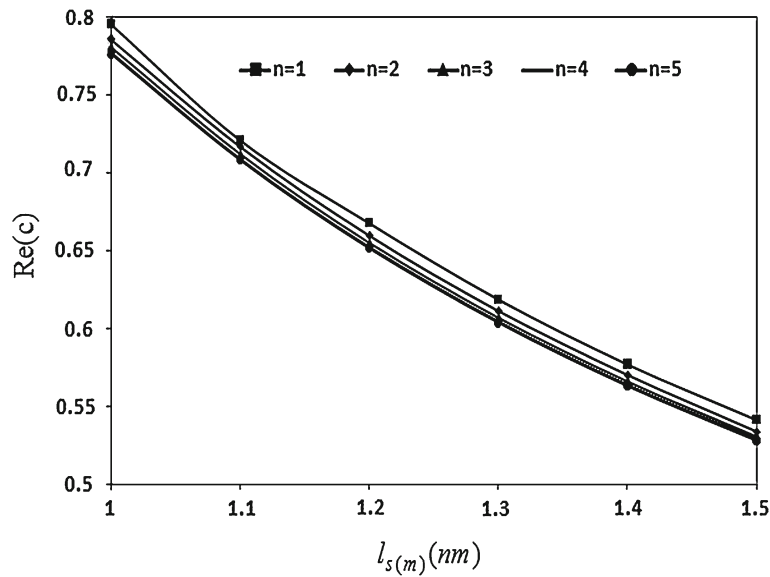


**Fig. 8** Dimensionless real part of  $c$  in terms of nonlocal parameter of nano-rod for different power index for  $V_0 = 10$  V and  $H_0 = 10$  A

Shown in Figs. 5 and 6 are the dimensionless imaginary part of the phase velocity  $c$  in terms of the wave number for different values of the power index for  $V_0(H_0) = 10$  V(A) and  $V_0(H_0) = 5$  V(A), respectively. It can be concluded that with increasing the power index  $n$ , and wave number  $k$ , the imaginary part increases.

To study the effect of nonlocal parameters of unified nonlocal elasticity ( $l_s, l_m$ ), a numerical analysis is performed for different values of nonlocal parameter and power index when two parameters are assumed identical ( $l_s = l_m$ ). Figures 7 and 8 show the dimensionless real part of the phase velocity in terms of the nonlocal parameter for different values of the power index for  $V_0 = H_0 = 5$  and  $V_0 = H_0 = 10$ , respectively. It is concluded that increasing the nonlocal parameter decreases the phase velocity considerably. The trend of these results is in accordance with the literature [26,27].

#### 4 Conclusion

In this study, a nonlocal elasticity solution was developed for the analysis of wave propagation in a functionally graded magneto-electro-elastic nano-rod subjected to two-dimensional electric and magnetic potentials. The effect of important parameters such as nanoscale parameters, applied voltage and and magnetic field, wave number and power index was investigated on the real and imaginary part of the phase velocity. Some important results of this paper are expressed as follows:

1. Investigation on the distribution of the real part of the phase velocity  $c$  in terms of different values of power index and wave number indicates that increasing the wave number and power index leads to a decreasing real part of  $c$ . The important reason for decreasing the phase velocity is a decreasing stiffness of the material along the longitudinal direction.
2. The distribution of the of imaginary part of phase velocity in terms of wave number and power index shows that for  $n = 2$ , the phase velocity has a minimum value. Increasing the wave number leads to increasing phase velocity.
3. The applied voltage and magnetic field play an important role in changing the imaginary part of the phase velocity of the nano-rod. Investigation on the distribution of the imaginary part of the phase velocity for different values of applied magnetic field and voltage indicates that increasing the applied voltage and magnetic field decreases considerably the dimensionless imaginary part of the phase velocity.
4. Nonlocal parameters of unified nonlocal elasticity theory have a considerable effect on the change of the phase velocity. The numerical results indicate that the phase velocity is decreased with increasing the nonlocal parameters of the nano-rod.

**Acknowledgments** The research described in this paper was financially supported by the University of Kashan (Grant Number: 463865/17) and Iranian Nanotechnology Development Committee. I would like to thank Dr. Loghman for language editing of this paper.

#### Appendix

$$\begin{aligned}
 A &= \int_{-\frac{b}{2}}^{+\frac{b}{2}} \int_{-\frac{h}{2}}^{+\frac{h}{2}} \rho dx_2 dx_3, B = \int_{-\frac{b}{2}}^{+\frac{b}{2}} \int_{-\frac{h}{2}}^{+\frac{h}{2}} \rho v^2 (x_2^2 + x_3^2) dx_2 dx_3, \\
 C &= \frac{1}{2} b \int_{-\frac{h}{2}}^{+\frac{h}{2}} l_m^2 \left\{ \rho (1 + 2\nu) + \nu x_3 \frac{\partial \rho}{\partial x_3} \right\} dx_3, D = \frac{1}{2} b \int_{-\frac{h}{2}}^{+\frac{h}{2}} E(x_3) dx_3, \\
 E &= -\frac{1}{2} b \int_{-\frac{h}{2}}^{+\frac{h}{2}} l_s^2 E(x_3) dx_3, F = \frac{1}{2} b \int_{-\frac{h}{2}}^{+\frac{h}{2}} e_{111} \left( \frac{1}{2} + \frac{z}{h} \right)^e V_0, \\
 G &= \frac{1}{2} b \int_{-\frac{h}{2}}^{+\frac{h}{2}} e_{113} \frac{e}{h} \left( \frac{1}{2} + \frac{z}{h} \right)^{e-1} V_0, H = \frac{1}{2} \int_{-\frac{b}{2}}^{+\frac{b}{2}} \int_{-\frac{h}{2}}^{+\frac{h}{2}} l_m^2 \rho v^2 [x_2^2 + x_3^2] dx_2 dx_3, \\
 I &= \frac{1}{2} \int_{-\frac{b}{2}}^{+\frac{b}{2}} \int_{-\frac{h}{2}}^{+\frac{h}{2}} \frac{E}{2(1+\nu)} v^2 [x_2^2 + (x_3)^2] dx_2 dx_3, \\
 J &= -\frac{1}{2} \int_{-\frac{b}{2}}^{+\frac{b}{2}} \int_{-\frac{h}{2}}^{+\frac{h}{2}} l_s^2 \frac{E}{2(1+\nu)} v^2 [x_2^2 + (x_3)^2] dx_2 dx_3, K = \frac{1}{2} b \int_{-\frac{h}{2}}^{+\frac{h}{2}} e_{111} \left( \frac{1}{2} + \frac{z}{h} \right)^e V_0 dx_3, \\
 L &= \frac{1}{2} b \int_{-\frac{h}{2}}^{+\frac{h}{2}} -\eta_{11} \left( \frac{1}{2} + \frac{z}{h} \right)^{2e} V_0^2 dx_3, \\
 M &= \frac{1}{2} b \int_{-\frac{h}{2}}^{+\frac{h}{2}} -\eta_{33} \left( \frac{e}{h} \right)^2 \left( \frac{1}{2} + \frac{z}{h} \right)^{2e-2} V_0^2 dx_3, N = -\frac{1}{2} b \int_{-\frac{h}{2}}^{+\frac{h}{2}} [\eta_{13} + \eta_{31}] \frac{e}{h} \left( \frac{1}{2} + \frac{z}{h} \right)^{2e-1} V_0^2 dx_3, \\
 O &= \frac{1}{2} b \int_{-\frac{h}{2}}^{+\frac{h}{2}} e_{311} \frac{e}{h} \left( \frac{1}{2} + \frac{z}{h} \right)^{e-1} V_0 dx_3,
 \end{aligned}$$

$$\begin{aligned}
P &= \frac{1}{2}b \int_{-\frac{h}{2}}^{+\frac{h}{2}} q_{11} \left(\frac{1}{2} + \frac{z}{h}\right)^e H_0 dx_3, \quad Q = \frac{1}{2}b \int_{-\frac{h}{2}}^{+\frac{h}{2}} q_{13} \frac{e}{h} \left(\frac{1}{2} + \frac{z}{h}\right)^{e-1} H_0 dx_3, \quad R = -\frac{1}{2}b \int_{-\frac{h}{2}}^{+\frac{h}{2}} \beta_{11} T dx_3, \\
S &= -\frac{1}{2}b \int_{-\frac{h}{2}}^{+\frac{h}{2}} g_{31} \frac{e}{h} \left(\frac{1}{2} + \frac{z}{h}\right)^{2e} H_0 V_0 dx_3, \quad U = -\frac{1}{2}b \int_{-\frac{h}{2}}^{+\frac{h}{2}} g_{33} \left(\frac{e}{h}\right)^2 \left(\frac{1}{2} + \frac{z}{h}\right)^{2e-2} H_0 V_0 dx_3, \\
V &= -\frac{1}{2}b \int_{-\frac{h}{2}}^{+\frac{h}{2}} p \left(\frac{e}{h}\right) \left(\frac{1}{2} + \frac{z}{h}\right)^{e-1} V_0 dx_3, \quad W = \frac{1}{2}b \int_{-\frac{h}{2}}^{+\frac{h}{2}} q_{111} \left(\frac{1}{2} + \frac{z}{h}\right)^e H_0 dx_3, \\
X &= -\frac{1}{2}b \int_{-\frac{h}{2}}^{+\frac{h}{2}} g_{11} \left(\frac{1}{2} + \frac{z}{h}\right)^{2e} H_0 V_0 dx_3, \quad Y = -\frac{1}{2}b \int_{-\frac{h}{2}}^{+\frac{h}{2}} g_{13} \left(\frac{e}{h}\right) \left(\frac{1}{2} + \frac{z}{h}\right)^{2e-1} H_0 V_0 dx_3, \\
Z &= -\frac{1}{2}b \int_{-\frac{h}{2}}^{+\frac{h}{2}} \mu_{11} \left(\frac{1}{2} + \frac{z}{h}\right)^{2e} H_0^2 dx_3, \quad A_1 = -\frac{1}{2}b \int_{-\frac{h}{2}}^{+\frac{h}{2}} \mu_{13} \left(\frac{e}{h}\right) \left(\frac{1}{2} + \frac{z}{h}\right)^{2e-1} H_0^2 dx_3, \\
B_1 &= -\frac{1}{2}b \int_{-\frac{h}{2}}^{+\frac{h}{2}} m \left(\frac{e}{h}\right) \left(\frac{1}{2} + \frac{z}{h}\right)^e H_0 dx_3, \quad C_1 = \frac{1}{2}b \int_{-\frac{h}{2}}^{+\frac{h}{2}} q_{311} \left(\frac{e}{h}\right) \left(\frac{1}{2} + \frac{z}{h}\right)^{e-1} H_0 dx_3, \\
D_1 &= -\frac{1}{2}b \int_{-\frac{h}{2}}^{+\frac{h}{2}} g_{31} \left(\frac{e}{h}\right) \left(\frac{1}{2} + \frac{z}{h}\right)^{2e-1} V_0 H_0 dx_3, \quad E_1 = -\frac{1}{2}b \int_{-\frac{h}{2}}^{+\frac{h}{2}} g_{33} \left(\frac{e}{h}\right)^2 \left(\frac{1}{2} + \frac{z}{h}\right)^{2e-1} V_0 H_0 dx_3, \\
F_1 &= -\frac{1}{2}b \int_{-\frac{h}{2}}^{+\frac{h}{2}} \mu_{31} \left(\frac{e}{h}\right) \left(\frac{1}{2} + \frac{z}{h}\right)^{2e-1} H_0^2 dx_3, \quad G_1 = -\frac{1}{2}b \int_{-\frac{h}{2}}^{+\frac{h}{2}} g_{33} \left(\frac{e}{h}\right) \left(\frac{1}{2} + \frac{z}{h}\right)^{2e-1} H_0^2 dx_3, \\
H_1 &= -\frac{1}{2}b \int_{-\frac{h}{2}}^{+\frac{h}{2}} m \left(\frac{e}{h}\right) \left(\frac{1}{2} + \frac{z}{h}\right)^{e-1} H_0 dx_3.
\end{aligned}$$

## References

1. Arefi, M.: Nonlinear thermoelastic analysis of thick-walled functionally graded piezoelectric cylinder. *Acta Mech.* **224**, 2771–2783 (2013)
2. Arefi, M., Rahimi, G.H.: Application of shear deformation theory for two dimensional electro-elastic analysis of a FGP cylinder. *Smart Struct. Syst.* **13**(1), 1–24 (2014)
3. Arefi, M., Khoshgoftar, M.J.: Comprehensive piezo-thermo-elastic analysis of a thick hollow spherical shell. *Smart. Struct. Syst.* **14**(2), 225–246 (2014)
4. Arefi, M., Nahas, I.: Nonlinear electro thermo elastic analysis of a thick spherical functionally graded piezoelectric shell. *Compos. Struct.* **118**, 510–518 (2014)
5. Ashida, F., Tauchert, T.R.: Thermally-induced wave propagation in a piezoelectric plate. *Acta. Mech.* **161**(1), 1–16 (2003)
6. Assadi, A., Farshi, B.: Size-dependent longitudinal and transverse wave propagation in embedded nanotubes with consideration of surface effects. *Acta. Mech.* **222**(1), 27–39 (2011)
7. Babaei, M.H., Chen, Z.T.: Exact solutions for radially polarized and magnetized magneto-electroelastic rotating cylinders. *Smart Mater. Struct.* **17**, 025035 (11pp) (2008)
8. Chen, W.Q., Wu, B., Zhang, C.L., Zhang, Ch: On wave propagation in anisotropic elastic cylinders at nanoscale: surface elasticity and its effect. *Acta. Mech.* **225**(10), 2743–2760 (2014)
9. Eringen, A.C.: On differential equations of nonlocal elasticity and solutions of screw dislocation and surface waves. *J. Appl. Phys.* **54**, 4703–4710 (1983)
10. Hadi, A., Daneshmehr, A.R.N., Mehrian, S.M., Hosseini, M., Ehsani, F.: Elastic analysis of functionally graded Timoshenko beam subjected to transverse loading. *Tech. J. Eng. Appl. Sci.* **3**(13), 1246–1254 (2013)
11. He, S.-r., Guan, Q.: Three dimensional analysis of piezoelectric/piezomagnetic and elastic media. *Compos. Struct.* **72**(4), 419–428 (2006)
12. Hsu, M.H.: Electromechanical analysis of piezoelectric laminated composite beams. *J. Mar. Sci. Tech.* **13**(2), 148–155 (2005)
13. Ikeda, T.: A piezomagnetic analysis of magnetoelastic waves in a ferromagnetic thin film. *Jpn. J. Appl. Phys.* **26**(7), Part1, 1014–1025 (1987)
14. Khoshgoftar, M. J. G Arani, A., Arefi, M.: Thermoelastic analysis of a thick walled cylinder made of functionally graded piezoelectric material. *Smart Mater. Struct.* **18**, 115007 (8pp) (2009)
15. Kuo W-Sh, Huang J.H.: The analysis of piezoelectric/piezomagnetic composite materials containing ellipsoidal inclusions. *J. Appl. Phys.* **81**, 1378–1389 (1997)
16. Ghorbanpour Arani, A., Shiravand, A., Rahi, M., Kolahchi, R.: Nonlocal vibration of coupled DLGS systems embedded on Visco-Pasternak foundation. *Phys. B* **407**, 4123–4131 (2012)

17. Ghorbanpour Arani, A., Shokravi, M., Amir, S., Mozdianfard, M.R.: Nonlocal electro-thermal transverse vibration of embedded fluid-conveying DWBNNTs. *J. Mech. Sci. Tech.* **26**(5), 1455–1462 (2012)
18. Güven, U.A.: Generalized nonlocal elasticity solution for the propagation of longitudinal stress waves in bars. *Eur. J. Mech. A. Solids* **45**, 75–79 (2014)
19. Güven, U.: A more general investigation for the longitudinal stress waves in microrods with initial stress. *Acta Mech.* **223**(9), 2065–2074 (2012)
20. Lu, B.P., Zhang, P.Q., Lee, H.P., Wang, C.M., Reddy, J.N.: Non-local elastic plate theories. *Proc. R. Soc. A* **463**, 3225–3240 (2007)
21. Nami, M.R., Janghorban, M.: Static analysis of rectangular nanoplates using trigonometric shear deformation theory based on nonlocal elasticity theory. *Beilstein J. Nanotechnol.* **4**, 968–973 (2013)
22. Mohammadimehr, M., Rahmati, A.H.: Small scale effect on electro-thermo-mechanical vibration analysis of single-walled boron nitride nanorods under electric excitation. *Turk. J. Eng. Environ. Sci.* **37**, 1–15 (2013)
23. Mohammadimehr, M., Saidi, A.R., Ghorbanpour Arani, A., Arefmanesh, A., Han, Q.: Buckling analysis of double-walled carbon nanotubes embedded in an elastic medium under axial compression using non-local Timoshenko beam theory. *Proc. Ins. Mech. Eng. C-J Mech.* **225**, 489–506 (2010)
24. Rahimi, G.H., Arefi, M., Khoshgoftar, M.J.: Electro elastic analysis of a pressurized thick-walled functionally graded piezoelectric cylinder using the first order shear deformation theory and energy method. *Mechanika* **18**(3), 292–300 (2012)
25. Santos, H., Soares, C.M.M., Soares, C.A., Reddy, J.N.: A finite element model for the analysis of 3D axisymmetric laminated shells with piezoelectric sensors and actuators: bending and free vibrations. *Comput. Struct.* **86**, 940–947 (2008)
26. Song, J., Shen, J., Li, X.F.: Effects of initial axial stress on waves propagating in carbon nanotubes using a generalized nonlocal model. *Comput. Mater. Sci.* **49**, 518–523 (2010)
27. Song, F., Huang, G.L., Varadan, V.K.: Study of wave propagation in nanowires with surface effects by using a high-order continuum theory. *Acta. Mech.* **209**, 129–139 (2010)
28. Wang, Q., Han, Q.K., Wen, B.C.: Estimate of material property of carbon nanotubes via nonlocal elasticity. *Adv. Theor. Appl. Mech.* **1**(1), 1–10 (2008)
29. Wu, Z.X., Hui, D.H.: Solution for a nonlocal elastic bar in tension. *Sci China Phys. Mech. Astron.* **55**(6), 1059–1065 (2012)
30. Yan, B.Z., Jiang, L.Y.: Vibration and buckling analysis of a piezoelectric nanoplate considering surface effects and in-plane constraints. *Proc. R. Soc. A* **468**, 3458–3475 (2012)